

Line-of-sight Effects on Observability of Kink Modes in Coronal Structures with Imaging Telescopes

F.C. Cooper, V.M. Nakariakov, D. Tsiklauri

Physics Department, University of Warwick, Coventry, CV4 7AL, England.

Received May 21, 2019/ Accepted ???? 2002

Abstract. Kink modes of solar coronal structures, perturbing the loop in the direction along the line-of-sight (LOS), can be observed as emission intensity disturbances propagating along the loop provided the angle between the LOS and the structure is not right. The phenomenon is based upon the change of the observed thickness of the loop (along the LOS) by the wave. The observed amplitude of the emission intensity variations can be larger than the actual amplitude of the wave by a factor of two. The observed amplitude depends upon the ratio of the wave length of kink perturbations to the width of the structure and on the angle between the LOS and the axis of the structure. This phenomenon should be taken into account in the interpretation of wave phenomena observed in the corona with space-borne and ground-based imaging telescopes.

Key words. Magnetohydrodynamics(MHD)– waves – Sun: activity – Sun: corona – Sun: oscillations – Sun UV radiation

1. Introduction

For last few years, a significant progress in the observational study of the MHD wave activity of the solar corona has been achieved with SOHO/EIT and TRACE EUV imaging telescopes. Flare-generated decaying oscillations of coronal loops have been observed and interpreted as kink fast magnetoacoustic modes of the loops (Aschwanden et al. 1999; Nakariakov et al. 1999; Schrijver & Brown 2000; Aschwanden et al. 2002). Fast magnetoacoustic waves have been found to be possibly responsible for such events as coronal Moreton (or EIT) waves (Thompson et al. 1998). Slow magnetoacoustic waves have been discovered in polar plumes (DeForest & Gurman 1998; Ofman, Nakariakov & DeForest 1999) and in long loops (Berghmans & Clette 1999; De Moortel, Ireland, Walsh 2000; Nakariakov et al. 2000; De Moortel 2002). This observational breakthrough gives rise to the implication of the method of MHD coronal seismology (Nakariakov et al. 1999; Robbrecht et al. 2001; Nakariakov & Ofman 2001) and supported wave-based theories of coronal heating (e.g., Tsiklauri & Nakariakov 2001), and the solar wind acceleration (e.g., Ofman, Nakariakov & Seghal 2000).

Slow and fast magnetoacoustic waves are compressive and cause perturbations of plasma density. As emission is proportional to the density, the waves can be detected as emission variations by imaging telescopes. An important

characteristic of the phenomenon is the angle between the direction of the wave propagation and the line of sight (LOS). Imaging telescopes allow one to observe magnetoacoustic waves propagating with a sufficiently high angle to the LOS. In particular, this fact motivated the interpretation of the propagating EUV emission disturbances as the slow magnetoacoustic waves (see the references above). In addition, Alfvén waves, which are linearly incompressible, as well as almost incompressible kink modes of coronal magnetic structures (e.g., Roberts 2000 and references therein), can also be detected with an imaging telescope, if perturbations of the magnetic field have a component *perpendicular* to the LOS. Indeed, as the magnetic field is frozen-in in the coronal plasma, the perpendicular displacement of the field can be highlighted by variation of emission intensity.

In this letter we discuss alternative way of the observational detection of kink modes of coronal magnetic structures, oscillating in the plane *containing* the LOS. It is shown that this would lead to modulation of the intensity of the emission *along the axis of the structure*, produced by the change of the observed thickness of the loop.

2. Kink modes of cylindric magnetic structures

Kink modes of coronal loops, observed, in particular, with TRACE EUV imaging telescope (see the references above), are periodic transverse displacements of the magnetic flux tube forming the loop. They should be distinguished from sausage modes which do not perturb the

tube axis. Modeling the loop tube as a straight magnetic cylinder uniform along the axis, Edwin & Roberts (1983) found that the kink modes can be either surface or body, depending upon the structure of the mode inside the tube. Also, the modes can be slow or fast, corresponding to fast and slow magnetoacoustic waves modified by the structuring of the medium. In particular, in the low- β plasma of the solar corona, coronal loops can support fast and slow kink body modes.

In the case of a kink mode, the loop tube oscillates almost as whole, and the cross-section of the loop is practically not perturbed by the oscillation. Also, the density perturbation inside the loop is insignificant in this mode. Indeed, for fast magnetoacoustic waves in a low- β coronal plasma, the field-aligned flows V_z are much smaller than the transverse motions V_x . Consequently, from the continuity equation, one gets that the density perturbations $\tilde{\rho}$ are connected with the transverse perturbations by the expression

$$\frac{\tilde{\rho}}{\rho_0} \approx \sqrt{1 - C_{A0}^2 k^2 / \omega^2} \frac{V_x}{C_{A0}}, \quad (1)$$

where ρ_0 and C_{A0} are the density and the Alfvén speed inside the loop tube, respectively, and other notations are standard. As the frequency ω of the fast kink mode of a coronal loop tends to the value $C_{A0}k$ with the increase of the wave number k (Edwin & Roberts 1983, Fig. 4), the coefficient on the right hand side of Eq. (1) tends to zero in the same limit. Consequently, the fast kink mode is almost incompressible. We would like to stress that the characteristic spatial scale of the mode *inside* the loop tube is quite different from the loop tube diameter. In the limit $\omega/k \rightarrow C_{A0}$, the characteristic transverse scale inside the tube tends to infinity. *Outside* the tube, the scale is different and it determines the mode localization length, which is about $\sqrt{\omega^2 / C_{Ae}^2 - k^2}$, where C_{Ae} is the Alfvén speed in the external medium. Consequently, outside the loop tube, the kink mode can be quite compressible.

The fast kink mode is often confused with the true incompressible Alfvén mode. However, actually, the Alfvén mode modified by structuring is the torsional mode which, in the linear limit, does not perturb the tube boundary.

Consider a kink mode which symmetrically perturbs the boundary of the loop tube. The wavelength is assumed to be much shorter than the loop length, so the loop can be considered as a straight cylinder. The plane of the transverse oscillations produced by the kink mode forms an angle α with the line-of-sight (LOS). In the following, we assume that the angle α is right. The tube axis has an angle θ with LOS (see Figure 1). We neglect the perturbations of density by the mode, assuming that the density is equal to the unperturbed density ρ_0 . The tube diameter is w . We also assume that the observed width of the tube does not change in time and space. The intensity of the emission i produced by the loop is proportional to the observed thickness of the loop tube l and to the density of the plasma squared,

$$i \propto \rho_0^2 l. \quad (2)$$

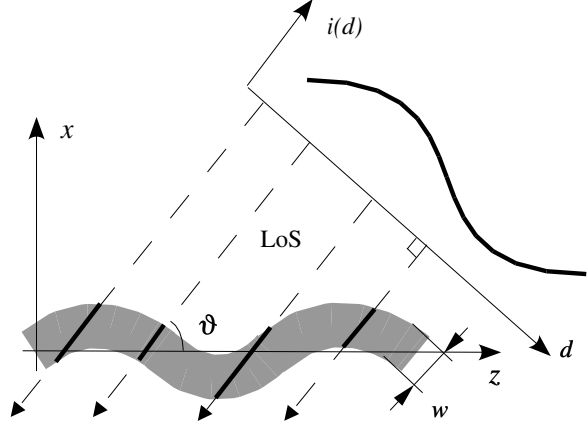


Fig. 1. A snapshot of perturbation of a segment of a coronal loop by a harmonic kink wave and produced variations of the emission intensity along the loop image. The variations produce the change of the observed thickness of the loop, if the angle θ between the loop axis and the line-of-sight differs from normal. The variations of the loop thickness modulate the emission intensity $i(d)$ on the loop image.

In the absence of the perturbations, the intensity i along a straight segment of the loop is constant, $i \propto \rho_0^2 w / \sin \theta$.

When the loop experiences kink perturbations, the observed thickness $l(d, t)$ of the loop tube depends upon the coordinate d along the loop (taking into account the effect of projection, see Fig. 1) and changes with time t . As, in the optically thin medium, the intensity of the emission is proportional to thickness of the volume of plasma emitting the radiation, the variation of the effective thickness causes the variation of the intensity. Thus, the emission intensity variations can be produced even by entirely *incompressible* kink waves, and, consequently, by the almost incompressible kink modes of coronal loops.

Note that the density perturbations produced by the wave outside the loop are ignored in Eq. (2), as the external plasma is observed to be much more rarefied.

3. Parametric studies

Consider a snapshot of a harmonic kink perturbation of a straight tube modeling a segment of a coronal loop. At a given time, boundaries of the tube are given by the equations

$$x = a \sin(kz) \pm \frac{w}{2}, \quad (3)$$

where a is the perturbation amplitude and k is the wave number ($k = 2\pi/\lambda$ where λ is the wavelength), and the plus and minus signs correspond to the upper and lower boundaries, respectively. The geometry of the problem is shown in Fig. 1. Observing the tube at an angle θ , we see that the observed thickness of the tube is modulated by

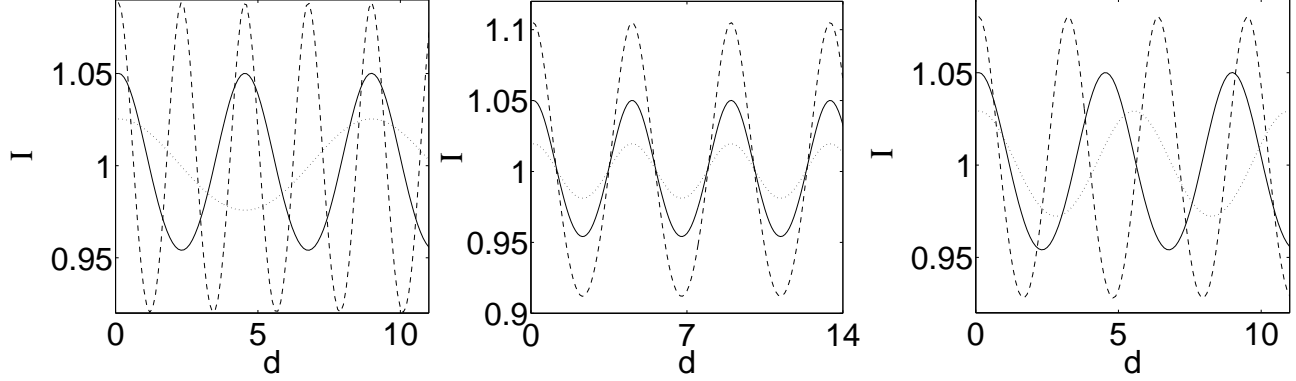


Fig. 2. Observed emission intensity variations along a straight segment of a coronal loop in the presence of a harmonic kink wave. The intensity I is normalized to the unperturbed intensity in the absence of the wave. The distance d is normalized to the loop radius. On the left panel, the dotted curve corresponds to the wavelength $\lambda = 4\pi$, the solid to $\lambda = 2\pi$ and the dashed to $\lambda = \pi$, measured in the loop radii. For all the curves, the normalized wave amplitude is $a = 0.05$ and the angle between the loop axis and the LOS is $\theta = \pi/4$. On the middle panel, the dotted curve corresponds to $a = 0.02$, the solid to $a = 0.05$ and the dashed to $a = 0.05$, for $\lambda = 2\pi$ and $\theta = \pi/4$. On the right panel, the dotted curve corresponds to $\theta = \pi/3$, the solid to $\theta = \pi/4$ and the dashed to $\theta = \pi/6$, for $a = 0.05$ and $\lambda = 2\pi$.

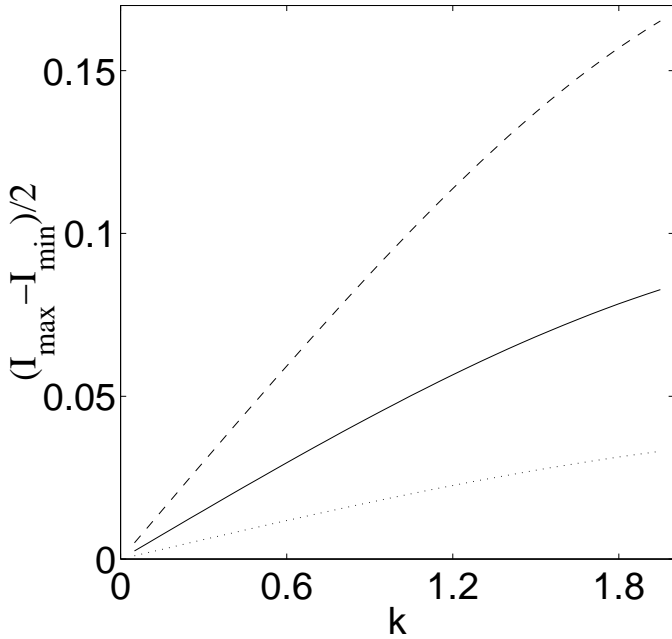


Fig. 3. Dependence of the observed amplitude of emission intensity variations along a straight segment of a coronal loop in the presence of a harmonic kink wave upon the wave number k , normalized to the loop radius. The dotted curve corresponds to the wave amplitude $a = 0.02$, the solid to $a = 0.05$ and the dotted to $a = 0.1$, for the angle between the loop axis and the LOS $\theta = \pi/4$.

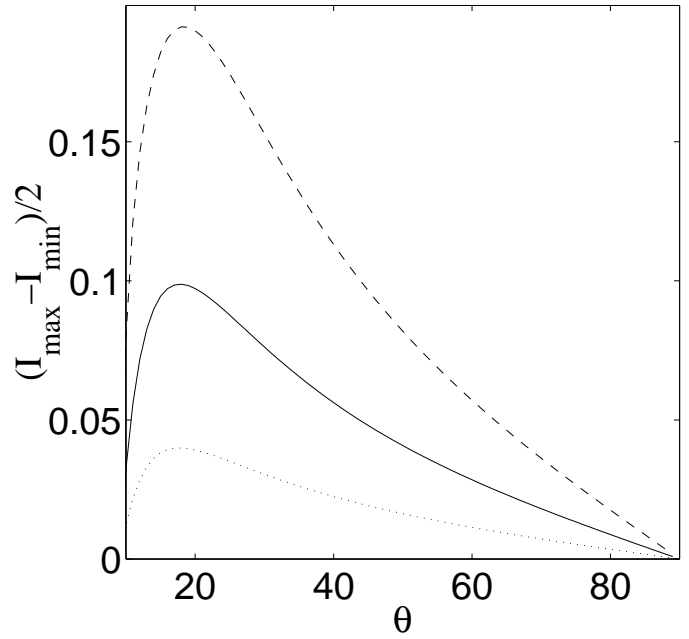


Fig. 4. Dependence of the observed amplitude of emission intensity variations along a straight segment of a coronal loop in the presence of a harmonic kink wave upon the angle between the loop axis and the LOS θ . The dotted curve corresponds to the wave amplitude $a = 0.02$, the solid to $a = 0.05$ and the dotted to $a = 0.1$, for the normalized wavelength $\lambda = 6\pi$.

the kink perturbation. The family of parallel LOS is given by the equation

$$x = z \tan \theta + d / \cos \theta, \quad (4)$$

where the parameter d represents the coordinate across the LOS and, consequently, along the image (see Fig. 1).

Solving the set of equations (3) and (4), we find the intersections of the LOS with the tube boundaries, and

determine the thickness of the tube along a given LOS as a function of the coordinate d along the image. Note that the line of sight may pass into and out of the flux tube more than once for certain amplitudes, LOS angles and wave numbers. We must therefore take into account all solutions of the set (3)-(4) and whether the line of sight is inside or outside of the tube. Thus, we determine the observed thickness of the tube as a function of the position

on the image, which, if the density of plasma inside the tube and the width of the tube across the LOS remain constant, is proportional to the intensity of the emission coming from the tube.

Figures 2-4 demonstrate how the effect discussed depends upon the parameters of the problem. Fig. 2 shows the distribution of the emission intensity along the tube on an image for different wavelengths and amplitudes of the kink mode and the observation angles θ . Obviously, the observed variation of the emission intensity is proportional to the amplitude of the wave and also inversely proportional to the wavelength. Indeed, in the limiting case when the wavelength tends to infinity, the observed thickness of the tube does not change and the effect vanishes. The dependence of the observed amplitude of the intensity perturbations upon the wave number of the kink wave is shown in Fig. 3. The observed amplitude is calculated as the difference between the maximum and the minimum values of the observed intensity, divided by two. The increase in the wave number (or decrease in the wavelength) amplifies the effect.

According to the right panel of Fig. 2 and Fig. 4, the dependence of observed amplitude of the intensity variations upon the angle θ is quite unexpected. Indeed, the effect of the modulation of the observed intensity by a kink wave vanishes when the angle tends to $\pi/2$, while the whole approach fails when $\theta \rightarrow 0$ (the leftmost data points in Fig. 4 correspond to $\theta = 10^\circ$). Fig. 4 clearly demonstrates, however, that there is an *optimal angle* which yields the maximum observed amplitude. Thus, this phenomenon would make it possible to observe kink modes in a certain segment of a coronal loop, where the angle θ is optimal.

4. Conclusions

The phenomenon of the modulation of the emission intensity by kink waves polarized in the plane formed by the loop axis and the LOS provides a possibility for the observational detection of the kink modes in coronal structures. According to the discussion above, the LOS effect can amplify the kink perturbations by a factor of 2. For example, if the boundary perturbation is produced by a kink mode of a relatively modest amplitude of about 5%, the observed perturbation of the intensity produced by the kink wave can reach 10%, which would make the wave easily observable. Additional observability constraints are connected with the wave period and length. In the case of EUV imaging coronal telescopes, such as EIT and TRACE, the observability of the waves is limited by the telescope time resolution. For example, taking the kink speed inside a loop to be 1000 km/s, the time resolution of about 30 s does not allow us to observe wavelengths shorter than 30 Mm. In the case of ground-based observations, when the loop is observed in the green line bandpass, the observability is limited by the spatial resolution of the telescope, which is usually over a few arcsec, as the time resolution of such observations is usually less than 1 sec. In both the cases, the

kink waves can be detected as emission intensity variations propagating along the loop by the stroboscopic method.

In particular, this effect can be responsible for propagating 6 second disturbances of the Fe XIV green line, discovered by the stroboscopic method in a solar eclipse data and interpreted as fast magnetoacoustic waves (Williams et al. 2002, see also Williams et al. 2001). The wavelength of these propagating disturbances is sufficiently small, probably just several times larger than the width of the loop, which makes the phenomenon discussed relevant to the interpretation. This subject will be discussed in more detail elsewhere.

Also, this phenomenon should be taken into account in the analysis of other examples of the coronal wave activity, in particular the slow waves in loops and polar plumes, discussed in Introduction. However, direct application of the results presented in this letter to the coronal slow magnetoacoustic waves is not possible as the slow waves are essentially compressible, and the density variation should be taken into account in Eq. (2). This phenomenon should also be taken into account in interpretation of intensity oscillations observed in prominence fine structures (e.g. Joarder, Nakariakov & Roberts 1997; Diaz et al. 2001). This suggests another possible way to development of this study.

Acknowledgements. FCC and DT acknowledge financial support from PPARC.

References

- Aschwanden M.J., De Pontieu B., Schrijver C.J., Title A.M., 2002, *Solar Phys.* 206, 99
- Aschwanden M.J., Fletcher L., Schrijver C.J. and Alexander D., 1999, *ApJ* 520, 880
- Berghmans D., Clette F., 1999, *Solar Phys.* 186, 207
- DeForest C.E., Gurman J. B., 1998, *ApJ* 501, L217.
- De Moortel I., Ireland J., Walsh R.W., 2000, *A&A* 355, L23
- De Moortel I., Hood A.W., Ireland J., Walsh R.W., 2002, *Solar Phys.* (in press)
- Díaz A.J., Oliver R., Erdélyi R., Ballester J.L., 2001, *A&A* 379, 1083
- Edwin P.M., Roberts B., 1983, *Solar Phys.* 88, 179.
- Joarder P.S., Nakariakov V.M., Roberts B., 1997, *Solar Phys.* 173, 81
- Nakariakov V.M., Ofman L., DeLuca E.E., Roberts B., Davila J.M., 1999, *Sci.* 285, 862
- Nakariakov V.M., Verwichte E., Berghmans D., Robbrecht E., 2000, *A&A* 362, 1151
- Ofman L., Nakariakov V.M., DeForest C.E., 1999, *ApJ* 514, 441
- Ofman L., Nakariakov V.M., Sehgal N., 2000, *ApJ* 533, 1071
- Robbrecht E., Verwichte E., Berghmans D., Hochedez J.F., Poedts S., Nakariakov V.M., 2001, *A&A* 370, 591
- Roberts B., 2000, *Solar Phys.* 193, 139
- Schrijver C.J., Brown D.S., 2000, *ApJ* 537, L69
- Thompson B.J., Plunkett S.P., Gurman J.B., Newmark J.S., St Cyr O.C., Michels D.J., 1998, *Geophys. Res. Lett.* 25, 2465
- Tsiklauri D., Nakariakov V.M., 2001, *A&A* 379, 1106
- Williams D.R., et al., 2001, *MNRAS* 326, 428
- Williams D.R., et al., 2002, *MNRAS* (in press)